Structural characterization and activation of nature's fuels of life

Rianne E. van Outersterp
Supervisors: Jonathan K. Martens and Anouk M. Rijs
Radboud University Nijmegen, Institute of Molecules and Materials, FELIX Laboratory
Contact: R.vanOutersterp@student.science.ru.nl

ABSTRACT
Hydrolysis of nucleotide triphosphates (NTPs) is known to drive highly important cellular processes. Of these NTPs, adenine triphosphate (ATP) is mainly studied as it is concerned to be the central fuel of living cells. Gas-phase studies have been performed to elucidate the conformational preference of NTPs focusing on the dependence of the nucleobase and extent of deprotonation. Therefore, a combination of infrared (IR) spectroscopy and mass spectrometry has been applied to ATP, CTP and GTP. IR action spectroscopy and supporting theoretical studies showed that the attached nucleobase has little influence on the three-dimensional structure of the phosphate tail. The favorable deprotonation sites of the singly and doubly deprotonated NTPs have been assigned. This can lead to a better explanation of the behavior and selection of NTPs in living cells.

Keywords
NTPs, ATP, CTP, GTP, CID, IRMPD, fragmentation channels, deprotonation sites, intramolecular H-bonding

INTRODUCTION
Nucleotide triphosphates (NTPs) drive central cellular processes such as nucleic acid synthesis, energy transfer, signaling processes and metabolism, which makes them indispensable factors for life. All NTPs consist of a nitrogen-containing base, a ribose and three phosphate groups (labeled α, β and γ) (Fig. 1). The different NTPs vary in their base, which is always a derivative of purine or pyrimidine [1]. Amongst the family of NPTs, adenosine 5'-triphosphate (ATP) takes an important place as ATP has been selected by nature to capture, transiently store and subsequently transfer energy to perform work in a cell [2, 3]. ATP has often been named the fuel that cells use to power their activities.
The chemical energy in ATP, and more generally in all NTPs, is stored in the covalent phosphodiester bonds linking the α-β and β-γ phosphate groups together, see Fig. 1. The most commonly occurring energy-releasing reaction in nature is the hydrolysis reaction in which the βγ-bond breaks, which yields a phosphate (P_i) and adenosine 5'-diphosphate (ADP). Cells use the energy released during this reaction to drive their activities by the protein-mediated coupling of this reaction to reactions that require energy [2,3].

SRC 2016, November 30, 2016, The Netherlands.

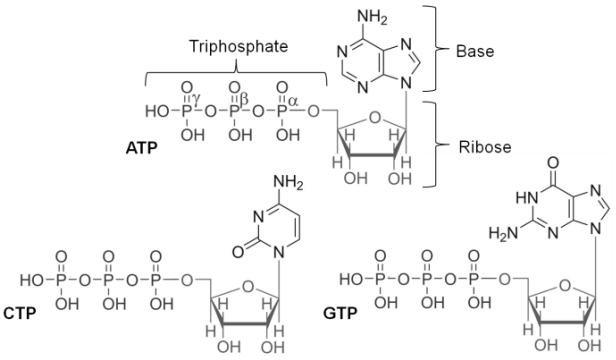

Figure 1. Chemical structures of ATP, CTP and GTP. The base, ribose and triphosphate are indicated. The standard labeling of the phosphate groups is shown.

The enormous importance for living organisms necessitates for a detailed insight in the structure and molecular mechanisms of this family of molecules. The function and recognition of a biomolecule is strongly related to its three-dimensional structure, which is a result of its internal covalent and non-covalent interactions. NTPs contain deprotonation sites at their α-, β- and γ-phosphates of which several are deprotonated at physiological pH. The resulting negative charge is stabilized by hydrogen bonds (H-bonds), which highly affects the molecules three-dimensional structure. Additionally, in biological situations, negative charges on NTPs are often stabilized by the interaction with metal cations [2].
Previous theoretical studies suggest that $[ATP\text{-}H]^{-1}$ is deprotonated at the α-phosphate [4], however, x-ray studies showed that metal cations mainly show interaction with the β- and γ-phosphates, which suggest that negative charge resides on these residues [2]. Theoretical studies suggest that $[ATP\text{-}2H]^{-2}$ shows αβ-deprotonation, which is confirmed by gas-phase infrared action spectroscopy [5]. Studies of NTP-binding aptamers shows that selective recognition of one NTP results from the nucleobase being the preferred recognition target. When, however, the triphosphate is recognized by the aptamers, binding of several NTPs is observed [6].
In the present work, also gas-phase experiments are performed, which offers the advantage to study the properties of biomolecules isolated from their crowded biological environment. Collision induced dissociation (CID) is performed to obtain insights into the fragmentation behavior of NTPs, while infrared multiple photon dissociation (IRMPD) spectroscopy in combination with quantum mechanical calculations is used to obtain structural information focusing on intramolecular H-bond interactions and deprotonation

sites. It is aimed to obtain detailed information about the intrinsic properties of deprotonated ATP and at the same time identify the similarities and differences with two other NTPs, Guanosine 5'-triphosphate (GTP) and Cytosine 5'-triphosphate (CTP) (Fig. 1).

EXPERIMENTAL

Experimental set-up

All experiments were performed in a modified commercial quadrupole ion trap mass spectrometer (Bruker, AmaZon Speed ETD) [7]. Ions were generated by electrospray ionization in an Apollo ESI source. Solutions of the NTPs (Sigma-Aldrich, disodium salt hydrates) of ~10^{-6} M (in 50:50 acetonitrile:water, ~2%) were introduced at 120 µl h^{-1} flow rates, electrosprayed and transferred into the trap. The ions of interest were mass-selected and fragmented, either by collision-induced dissociation (CID) or infrared-multiple photon dissociation (IRMPD).

Collision induced dissociation

Mass spectra (MS) after collision induced dissociation were recorded to obtain fragmentation patterns of the single and double anions. Ions were activated by 50 ms of CID with an amplitude parameter of 0.26. For each ion 12 mass spectra were recorded and averaged.

Infrared multiple-photon dissociation spectra

IRMPD spectra were recorded in the 400-1800 cm^{-1} region using the free electron laser FELIX at the FELIX laboratory. FELIX produced IR radiation in the form of 5-10 µs macropulses of 20-50 mJ at 5 Hz. The ions were irradiated with 2 macropulses. Resonant absorption of IR radiation leads to the increase of the internal energy of an ion due to intramolecular vibrational redistribution, which causes the ion to dissociate. At each wavelength, 5-6 mass spectra were recorded and averaged after irradiation. The dissociation yield at each wavelength is calculated by relating the precursor and fragment ion intensities (yield = $\Sigma I_{\text{fragment ions}} / (\Sigma I_{\text{parent ion}} + \Sigma I_{\text{fragment ions}})$). The yield was linearly corrected for wavelength-dependent laser power and the frequency was calibrated using a grating spectrometer.

Computational methods

In order to obtain optimized molecular geometries and predicted (linear) IR spectra of the singly and doubly deprotonated NTPs, density functional theory (DFT) calculations were performed (B3LYP, 6-31++G(d,p)) using Gaussian09 [8]. Input structures for the calculations of the double anions were defined as the $[ATP-2H]^{-2}$ structures calculated by Schinle et al. [5]. A molecular dynamics (MD) computational approach using AMBER 12 [9] was applied in order to find possible low energy structures for the mono-anions. After an initial minimization within AMBER, a simulated annealing procedure was used. Five hundred structures were obtained as snapshots throughout the procedure and grouped based on structural similarity. ~50 candidate structures obtained this way were calculated at the DFT level as described above.

Usually, these predicted vibrational spectra were scaled in the ~800-1800 cm^{-1} region using a linear scaling. However, previous studies of phosphate containing molecules have shown that P-O and P=O stretching modes provide a better match with the measured

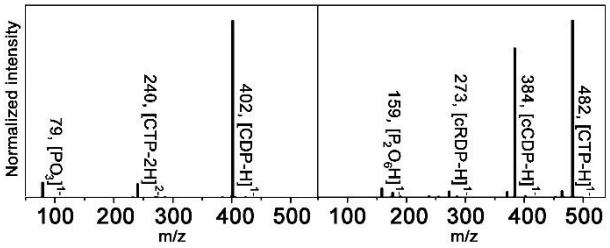

Figure 2. Fragmentation mass spectra of $[CTP-2H]^{2-}$ (left) and $[CTP-H]^{1-}$ (right). All peaks are labeled with the m/z-value and name.

spectrum when no scaling factor is used [10,11]. Therefore, phosphate bands were selected based on the absolute and relative displacement of the P and O atoms in the phosphate groups and not scaled, while other bands are scaled by 0.975. Below 800 cm^{-1} no scaling factor is applied. The vibrational stick spectra are broadened with a Gaussian line shape with 15 cm^{-1} full width at half maximum to facilitate comparison with experimental spectra.

RESULTS AND DISCUSSION

Fragmentation channels

CID MS/MS spectra of $[CTP-H]^{1-}$ or $[CTP-2H]^{2-}$ are shown in Fig. 2. $[CTP-2H]^{2-}$ shows mainly a hydrolysis-like fragmentation to phosphate (PO_3^{2-}) and deprotonated cytosine-5'-diphosphate ($[CDP-H]^{1-}$). For $[CTP-H]^{1-}$ mainly three CID fragments are observed. The m/z=384 peak is assigned to result from phosphate loss and subsequent cyclization, yielding cyclic CDP ($[cCDP-H]^{1-}$). The m/z=273 peak is assigned to be a cyclic ribose-diphosphate ($[cRDP-H]^{1-}$), resulting from the same phosphate loss and cyclization but with additional loss of the base. The m/z=159 peak is assigned to be a diphosphate ($P_2O_6H^-$), resulting from the breaking of the βγ-bond. Thus, at least three dominant fragmentation channels are observed for $[CTP-H]^{1-}$, whereby $[CTP-2H]^{2-}$ shows a dominant hydrolysis-like fragmentation pattern. This difference suggests that the extra charge present on $[CTP-2H]^{2-}$ helps in making the hydrolysis-reaction most favorable. For ATP and GTP similar results were obtained and are therefore not discussed here.

Comparisons of measured and calculated IR spectra of CTP

Singly deprotonated CTP

The recorded IR spectrum in the region between 450-1800 cm^{-1} of $[CTP-H]^{1-}$ is compared to the calculated IR spectra of the lowest energy conformers found for β-, γ- and α-deprotonated CTP (see Fig. 3). The calculated structures and energies relative to the ground-state conformer are inlayed for each plot. Besides their different deprotonation sites the structures differ in their H-bonding pattern and the orientation of the phosphate tail, while the conformation of the nucleobase and the sugar group remains virtually unchanged. A notable difference is that in the β- and γ-conformer the ribose group forms a H-bond with the γ -phosphate, while in the α-conformer this H-bond is formed with the β-phosphate. This results in a more compact structure for the α-conformer as compared to the more cyclic folded phosphate tail for the other two. The significant higher predicted energy of the α-conformer suggest that this cyclic conformation is more favorable.

All calculated spectra show some common features found

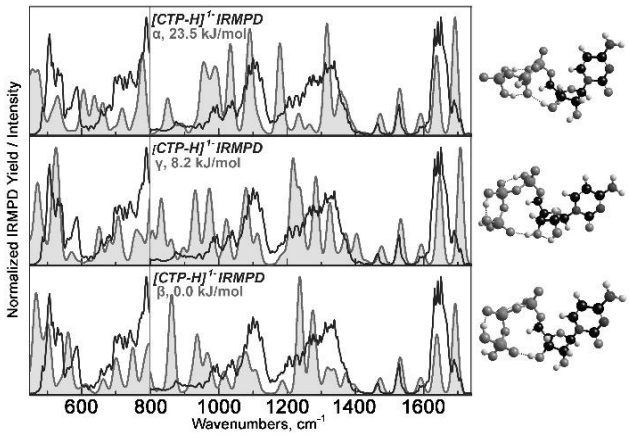

Figure 3: Comparisons between calculated (grey) and measured (black) IRMPD spectra of $[CTP\text{-}H]^{1-}$. Relative predicted energies and deprotonation sites are inlayed in the plots.

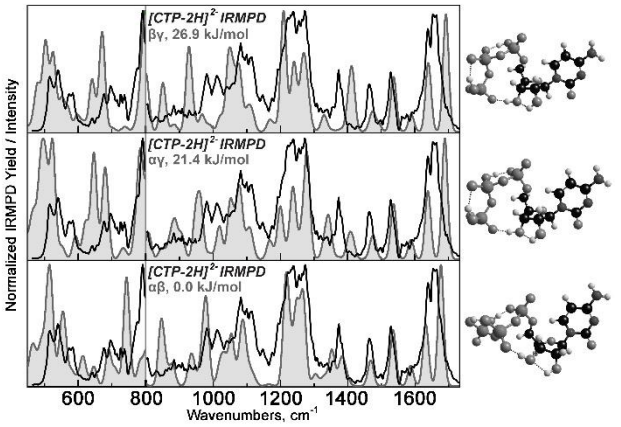

Figure 4: Comparisons between calculated (grey) and measured (black) IRMPD spectra of $[CTP\text{-}2H]^{2-}$. Relative predicted energies and deprotonation sites are inlayed in the plots.

in the experimental spectra, but differ in detail. Around 1650 cm^{-1} an intense band is observed with a small shoulder at the blue side. The main band is well predicted by all the calculations but the shoulder is predicted red-shifted for the γ-conformer. Besides, at 1400 cm^{-1} no intensity is observed while a band is predicted for this conformer. In the 1100-1400 cm^{-1} a broad band is measured which overlaps with a region of P=O stretches in all of the calculated spectra. However, the low intensity predicted around 1250 cm^{-1} for the α-conformer makes it, together with its high predicted energy, less likely that this conformer is present in the experiments. Both the β- and γ-conformers show a reasonable match and effectively only differ in their predicted relative intensities in this region. Between 950 and 1150 cm^{-1} three bands are observed. These three bands are slightly redshifted for the β- and γ-conformer and the shape of the measured band around 1100 cm^{-1} is predicted well for these conformers. In the 450-800 cm^{-1} region several closely spaced peaks are observed. Most of these peaks are consistent with the γ-conformer. However, the β-conformer shows a reasonable match in the sense that regions of high and low intensity are well predicted and when we take a small red-shift into account as in the previous region all bands are predicted by this conformer very well. The α-conformer does not match in this region. Based on this comparison, the assignment of one specific conformer is difficult and it has to be concluded that apparently both the β- and γ-conformer, differing only in the presence of one H-atom on either one side of a H-bond are present in the experiments. This is in agreement with the low energies predicted for these conformers.

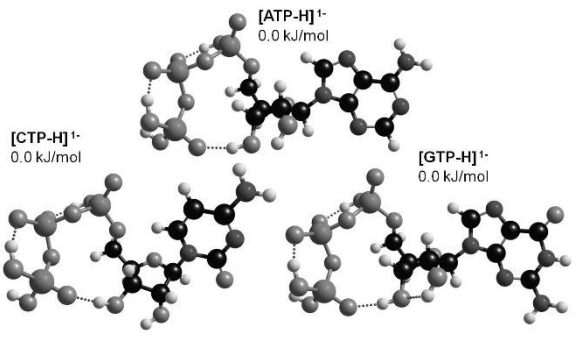

Figure 5: Assigned β-deprotonated structures for ATP, CTP and GTP. γ-deprotonated structures are also assigned to be present.

Doubly deprotonated CTP

Calculated IRMPD spectra of the lowest energy conformers found for αβ-, αγ- and βγ-deprotonated CTP are compared with the measured IRMPD spectrum of $[CTP\text{-}2H]^{2-}$ in Fig. 4. Calculated structures and relative energies are inlayed for each plot. Again, differences between the structures are, besides their different deprotonation sides, mainly found in the conformation and H-bonding of the phosphate tail. Also for the doubly deprotonated NPTs the H-bond between the ribose group and one of the phosphate groups has a large impact on the phosphate tail conformation. In the αβ-conformer the β-phosphate hydrogen bonds to the ribose group, leading to a structure comparable to α-deprotonated $[CTP\text{-}H]^{1-}$. In the αγ- and βγ-conformer the γ-phosphate is involved in the H-bond with the ribose, resulting in a structure comparable to the singly β- and γ-deprotonated CTP. In contrast to $[CTP\text{-}H]^{1-}$ it is interesting to note that the calculated energies indicate that the compact conformation is the most favorable.

The details providing distinction of these structures are discussed below. Around 1400 cm^{-1} a feature is observed which is well predicted by the calculation to be a ribose vibration of the αβ-conformer. However, this peak is blue shifted for the αγ- and βγ- conformer due to the different H-bond interaction. Overall, the calculated spectrum of the αβ-conformer shows a better match with the experimental spectrum. Just above 1200 cm^{-1} a broad band is measured which overlaps with a region of P=O stretches in all of the calculated spectra. However, the shape of the band matches better with the αβ-conformer. Between 900 and 1200 cm^{-1} a number of bands are observed in the calculated spectra

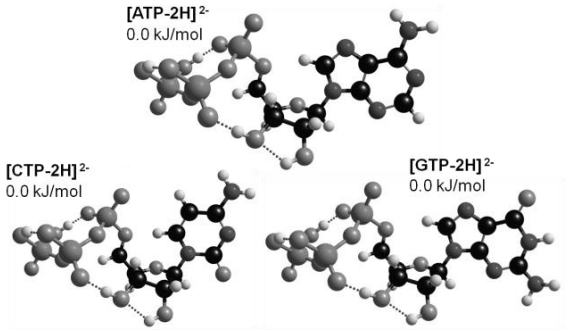

Figure 6: Assigned structures for double deprotonated ATP, CTP and GTP. All structures are deprotonated at the αβ-phosphate.

which appear to be red shifted compared to the experiment. Though, this shift is reasonably small for the αβ-conformer and larger for the other conformers. The pattern observed between 450 and 800 cm^{-1} is generally better represented in the calculated spectrum of the αβ-conformer, which makes this region consistent with the other observations.

Based on the above comparison, the αβ-conformer is assigned to have the largest contribution in the experiments. This in agreement with the low energy predicted for this conformer.

Comparisons of CTP, ATP and GTP

The above analysis has also been performed on singly and doubly deprotonated ATP and GTP and let to analogous conclusions. The assigned structures for all singly and doubly deprotonated NTPs are shown in Fig. 5 and Fig. 6, respectively. The assigned structures show similarities for both the singly and doubly deprotonated anions, which is especially clear when regarding the global positions of the atoms in the phosphate tail and their H-bonding interactions.

CONCLUSION, DISCUSSION AND OUTLOOK

The mass spectra show that activation of doubly deprotonated NTPs show dominantly hydrolysis-like fragmentation, while the singly deprotonated anions show multiple fragmentation channels. This suggests that the multiple charges present on NTPs in biological situations play a role in their hydrolysis reactions.

Infrared action spectroscopy and supporting theoretical studies have been performed to obtain structural information of singly and doubly deprotonated CTP, ATP and GTP. The spectra and calculations support the conclusion that the doubly deprotonated anions show mainly αβ-deprotonation. This is in agreement with previous studies. It was not possible to assign a single dominant deprotonation scheme for the singly deprotonated anions. However, since the β- and γ-conformers are highly similar it is likely that both conformers are present in the experiments. This is in contradiction with previous theoretical studies, however the present results might explain the previously observed interaction of metal cations with both the β- and γ-phosphates.

The difference in favored deprotonation sites observed for singly and doubly deprotonated NTPs might be explained by the fact that αβ-deprotonation favors a more compact structure with stronger hydrogen-bonds. This might help in the stabilization of the two charges present on the phosphate tail in the absence of stabilization by metal cations.

The assigned structures suggest that the three-dimensional structure and intramolecular H-bonding of the phosphate tail is highly similar for CTP, ATP and GTP. This suggests that the nucleobase that is attached has little to no influence on the three-dimensional structure of the phosphate tail. This might explain why triphosphate recognizing aptamers show no selective binding of a specific NTP. Besides it suggests that biological systems that do recognize specific NTPs do this solely via the nucleobase [6].

Additional experiments on the structural differences between NTPs could give further information about their selective recognition and different roles in a living cell. As NTPs often form complexes with one or more metal cations, proteins often recognize the metal complexes of NTPs. Infrared action spectroscopy on metal bound NTPs would therefore be an important next step to gain more insight in the properties of specific NTPs.

ROLE OF THE STUDENT

Rianne van Outersterp was an undergraduate student working under the supervision of Jonathan Martens and Anouk Rijs when the research in this report was performed. The topic was proposed by A.R. IRMPD experiments were performed by the student and J.M. CID experiments were performed by the student. Analysis of the results, formulation of the conclusions and writing of the report were done by the student.

REFERENCES

1. Bowater, R.P. & Gates, A.J. Nucleotides: Structure and properties. In: Encyclopedia of Life Sciences, John Wiley & Sons (2005)
2. Cohn, M. Adenosine triphosphate, In: Encyclopedia of Life Sciences, John Wiley & Sons (2001)
3. Lodish, H. et al. *Molecular cell biology*, Vol. 7. W.H. Freeman New York (2012), 52-54
4. Burke, R.M. et al. Stabilization of Excess Charge in Isolated Adenosine-5'-Triphosphate and Adenosine 5'-Diphosphate Multiply and Singly Charges Anions. *J. Phys. Chem. A*, 109 (2005), 9775-9785
5. Schinle, F. et al. Spectroscopic and theoretical investigations of adenosine 5'-diphosphate and adenosine 5'-triphosphate dianions in the gas phase. *Physical Chemistry Chemical Physics 15*, 18 (2013), 6640-6650
6. Sazani, P.L. et al. A Small Aptamer with Strong and Specific Recognition of the Triphosphate of ATP. *J. Am. Chem. Soc.*, 126 (2004), 8370-8371
7. Martens, J.K. et al. Structural identification of electron transfer dissociation products in mass spectrometry using infrared ion spectroscopy. *Nature Communications 7*, 11754 (2016) doi: 10.1038/ncomms11754
8. Frisch, M.J. et al. Gaussian 09 (Gaussian, Inc., Wallingford, CT, 2009).
9. Case, D.A. et al. AMBER 12 (University of California, San Francisco, CA, 2012).
10. Nei, Y.W., et al. Infrared multiple photon dissociation action spectroscopy of deprotonated DNA mononucleotides: gas-phase conformations and energetic. *The Journal of Physical Chemistry A 117*, 6 (2013), 1319-1335
11. Fales, B.S., et al. Infrared multiple photon dissociation action spectroscopy and theoretical studies of diethyl phosphate complexes: Effects of protonation and sodium cationization on structure. *Journal of the American Society for Mass Spectrometry 22*, 1 (2011), 81-92